Pregnane X Receptor Regulates Liver Size and Liver Cell Fate via Yes-associated Protein Activation

Yiming Jiang[1], Dechun Feng[2], Xiaochao Ma[3], Shicheng Fan[1], Yue Gao[1] Kaili Fu[1], Ying Wang[4], Jiahong Sun[1], Xinpeng Yao[1], Conghui Liu[1], Huizhen Zhang[1], Leqian Xu[1], Aiming Liu[5], Frank J. Gonzalez[6], Yingzi Yang[7], Bin Gao[2], Min Huang[1], Huichang Bi[1*]

[1]Guangdong Provincial Key Laboratory of New Drug Design and Evaluation, School of Pharmaceutical Sciences, Sun Yat-Sen University, Guangzhou, China

[2]Laboratory of Liver Diseases, National Institute on Alcohol Abuse and Alcoholism, National Institutes of Health, Bethesda, Maryland, USA

[3]Department of Pharmaceutical Sciences, School of Pharmacy, University of Pittsburgh, Pittsburgh, Pennsylvania, USA

[4]Sun Yat-sen Memorial Hospital, Sun Yat-sen University, Guangzhou, China
[5]Medical School of Ningbo University, Ningbo, China

[6]Laboratory of Metabolism, Center for Cancer Research, National Cancer Institute, National Institutes of Health, Bethesda, Maryland, USA

[7]Harvard School of Dental Medicine, Boston, MA, USA

Supplementary Materials and Methods

Mouse treatments

The treatment strategy in wild-type (WT) and *Pxr*-null mice was previously described (1). Briefly, 8- to 9-week-old male C57BL/6 mice were *i.p.* injected with vehicle (corn oil, Sigma, St. Louis, MO) or 100 mg/kg PCN (Sigma, St. Louis, MO) every day. Livers were harvested at 12 h after the last injection. For PXR-humanized (*hPXR*) mice, 8- to 9-week-old male *hPXR* mice had access to food and water ad libitum. Eight Mice were divided into two groups and either fed standard diet or the diet containing 100 mg/kg of rifampicin (RIF, Sigma, St. Louis, MO). A two-thirds partial hepatectomy (PHx) was carried out as previously described (2). Following two-thirds PHx, WT mice were *i.p.* injected with vehicle (corn oil) or 100 mg/kg/d PCN. Tissues were harvested at 1, 2, 3, 5 and 7 days after surgery and livers and body weights were measured. After two-thirds PHx，*hPXR* mice were gavaged with vehicle (0.5% CMC-Na) or 50 mg/kg/d RIF. Tissues were harvested at 2 and 5 days after surgery. A portion of liver was immediately fixed in 10% buffered formalin for histological section. The remaining tissue was flash frozen in liquid nitrogen and stored at -80ºC for further use.

Cell fate tracing. As previously described, *Sox9-Cre*^{ERT} mice were crossed with *Rosa26*^{EYFP} reporter mice to track bile duct cells/liver progenitor cells (3). To achieve Cre-LoxP recombination, tamoxifen (TAM, Sigma, St. Louis, MO) dissolved in corn oil at a concentration of 10 mg/mL was injected *i.p.* at 50 mg/kg body weight every 3 days for 3 times. Mice were subjected to PCN injection 7 days after TAM injections. To label hepatocytes, *Rosa26*^{EYFP} reporter mice were infected with adeno-associated virus (AAV)-thyroid-binding globulin (*Tbg*)-Cre (1.3×10^{11} genome copies per mouse, Penn Vector Core, Philadelphia, PA) by *i.v.* injection. Mice were subjected to PCN injection 10 days after AAV injections.

YAP interference

Eight- to 9-week-old male C57BL/6 mice were infected with AAV-Control-EGFP or AAV-*Yap*-shRNA-EGFP (1.1×10^{11} genome copies per mouse, Hanbio Co. Ltd, Shanghai, China) by *i.v.* injection. Mice were subjected to PCN injection 4 weeks after AAV injection.

Histological and biochemical assessment

Immunohistochemical staining in the liver: Paraffin-embedded sections were stained with SOX9 antibody, YAP antibody, KI67 antibody from Cell Signaling Technology (Beverly, MA), MPO antibody from Biocare Medical (Concord, CA) and β-catenin antibody from BD Biosciences (San Jose, CA) after heat-induced epitope retrieval in citrate buffer (pH 6.0) and visualized by DAB.

Immunofluorescence staining: Mice tissues were obtained and fixed in formalin, and then were embedded in O.C.T and sectioned (10 μm). Sections were stained with SOX9 (rabbit monoclonal) antibody (Cell signaling Technology, MA, USA), SOX9 (mouse

monoclonal) antibody (Thermo Fisher Scientific, Waltham, MA), CYP2D6 antibody (Sigma, St. Louis, MO), ALBUMIN antibody (R&D Systems, MN, USA), EYFP antibody (Cell signaling Technology, MA, USA) and HNF4α antibody (Abcam,Cambridge, MA). Fluorescent labeled secondary antibodies (Cell Signaling Technology, MA, USA) were used to visualize the primary antibodies. Images were obtained by using LSM 710 confocal microscope (Zeiss, Thornwood, NY).

Hematoxylin and eosin staining: Liver tissues were fixed in neutral buffered formalin and embedded in paraffin. Fixed tissues were cut into 4 μm thick sections and stained with hematoxylin and eosin (H&E, Servicebio, Wuhan, China). H&E staining was pictured by NIKON ECLIPSE CI microscope (Nikon Instruments, Japan).

Biochemical evaluation: Levels of alanine transaminase (ALT), aspartate transaminase (AST), albumin (ALB) and total bilirubin (TBIL) in serum were determined to evaluate liver injury using a HITACHI 7020 automatic biochemical analyzer (Hitachi, Tokyo, Japan) and commercial reagent kit (Kehua Bio-engineering, Shanghai, China). Hepatic triglyceride and cholesterol levels were measured using a triglyceride and cholesterol assay Kit (Nanjing Jiancheng Bioengineering Institute, Nanjing, China).

Quantitative real-time PCR analysis

Total RNA was isolated using Trizol reagent (Invitrogen, Grand Island, NY, USA) and quantified by the NanoDrop spectrophotometer (Thermo Scientific, Rockford, IL, USA) as described previously (4). Complementary DNA was synthesized with 1μg of total RNA using a PrimeScript RT reagent kit (TaKaRa Biotech, Kyoto, Japan).SYBR Premix Ex Taq II kit (TaKaRa Biotech, Kyoto,Japan) was used to perform qRT-PCR mix. The amplification reaction was carried out in the ABI-Prism 7500 sequence detection system (Applied Biosystems, Foster City, CA). Results were normalized to mouse *Gapdh* mRNA. Gene-specific primers were obtained from a primer bank and sequences of primers were listed in Table S1.

Western blot analysis

Western blot was performed as described in our previous report (5). Briefly, protein extracts were prepared from liver tissue using RIPA lysis buffer (Biocolors, Shanghai, China) or Nuclear/Cytosol Extract kit (Sangon Tech, Shanghai, China). Protein extracts (40 μg protein/lane) were electrophoretically resolved using a polyacrylamide gel (8%-15% SDS gel) and transferred to a polyvinylidenefluoride membrane (0.2 μm, Millipore, Bedford; 0.45 μm, GE Healthcare Life Sciences, Piscataway, NJ). Blots were blocked for 1 h at room temperature with 5% BSA or 5% non-fat milk and then incubated with primary antibody overnight at 4 °C. Rabbit polyclonal anti-CCND1, anti-CDK4, anti-MST1, anti-MST2, anti-p-MST1/2 and anti-GAPDH antibodies were all purchased from Cell Signaling Technology (Cell Signaling Technology, MA, USA). Rabbit polyclonal anti-YAP antibody and anti-CYP3A antibody was acquired from Santa Cruz Biotechnology (Santa Cruz, CA, USA). Rabbit anti-phosphorylated YAP, anti-

ANKRD1, anti-CYR61, anti-CCNA1, anti-CCNE1, anti-GSTM2 and anti-LAMIN B antibodies were purchased from Sangon Biotechnology (Sangon Tech, Shanghai, China). Rabbit polyclonal anti-CTGF antibody was obtained from Proteintech (Proteintech, Wuhan, China). Rabbit polyclonal anti-LATS2 and anti-p-LATS1/2 antibody was obtained from Abcam (Abcam, UK). Peroxidase-conjugated anti-rabbit immunoglobulin G (IgG) antibody was purchased from Cell Signaling Technology (Cell Signaling Technology, MA, USA). Chemiluminescence was detected using the electrochemiluminescence detection kit (GE Healthcare Life Sciences, Piscataway, NJ).

Primary hepatocytes culture and co-immunoprecipitation (co-IP)

Primary hepatocytes from male C57BL/6 mice (8-9 weeks) were isolated and cultured according to the method described previously (6). Co-immunoprecipitation (co-IP) was performed using Thermo Scientific Pierce co-IP kit (Thermo Scientific, Rockford, IL) following the manufacturer's protocol. Samples were analyzed by Western blotting using anti-IgG (Merk, MA, USA), anti-PXR and anti-YAP (Santa Cruz, CA, USA).

HepG2 culture and co-localization

HepG2 cells (ATCC) were cultured in DMEM containing 10 % FBS. Cells were treated with DMSO or 20 μM RIF for 48 h. At indicated time points, cells were fixed in 4% paraformaldehyde for 30 min and 0.5% triton X-100 for 10 min at RT. Then, cells were incubated with Rabbit polyclonal anti-PXR (Santa Cruz, CA, USA) and mouse monoclonal anti-YAP (R&D Systems, MN, USA) overnight at 4 °C. Cells were stained with secondary antibodies including anti-mouse IgG Alexa Fluor 488 and anti-rabbit IgG Alexa Fluor 647 (Cell Signaling Technology, MA, USA). Images were acquired using a confocal microscope (Olympus FV3000, Japan).

AML12 culture and *Yap* interference

AML12 cells (ATCC, Manassas, VA) were cultured in DMEM/F12 containing 0.005 mg/mL insulin, 0.005 mg/mL transferrin, 5 ng/mL selenium 40 ng/mL dexamethasone and 10 % FBS. Cells were transfected with 10 μL of AAV Control or AAV *Yap* shRNA for 48 h. At 48 h after transfection, samples were analyzed by qRT-PCR.

Supplementary Figures

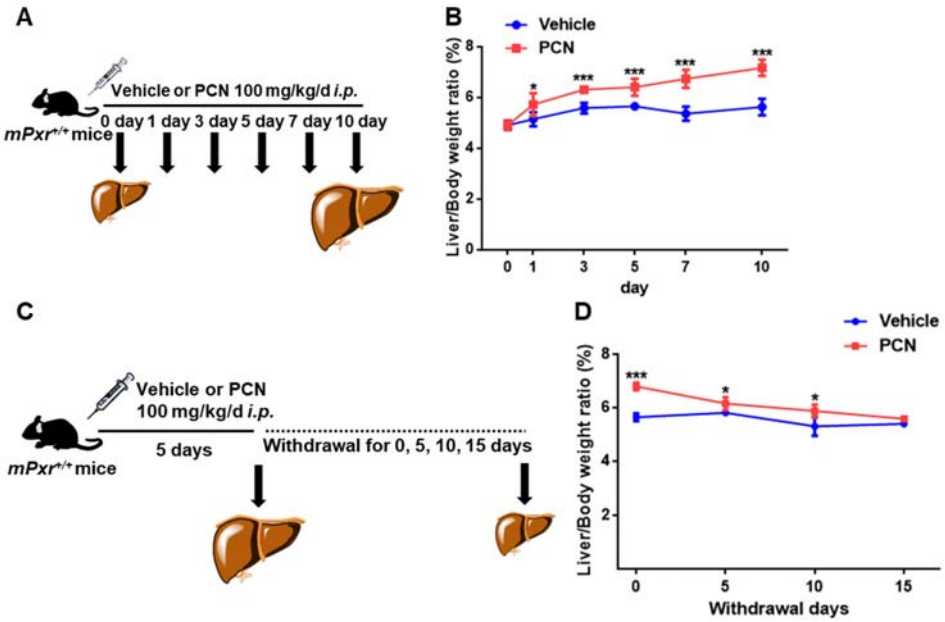

Figure S1. Effects of PCN-induced PXR activation on liver enlargement in WT mice. (A) WT mice were treated with vehicle (corn oil) or PCN (100 mg/kg/d) for 10 days. (B) Liver-to-body-weight ratios. (C) Mice were treated PCN (100 mg/kg/d) for 5 days and withdrawal for 0, 5, 10, 15 days. (D) Liver-to-body-weight ratios. Data were expressed as mean ± SD (n = 6). $^{*}P$<0.05 and $^{***}P$<0.001 compared to vehicle group at the same time point.

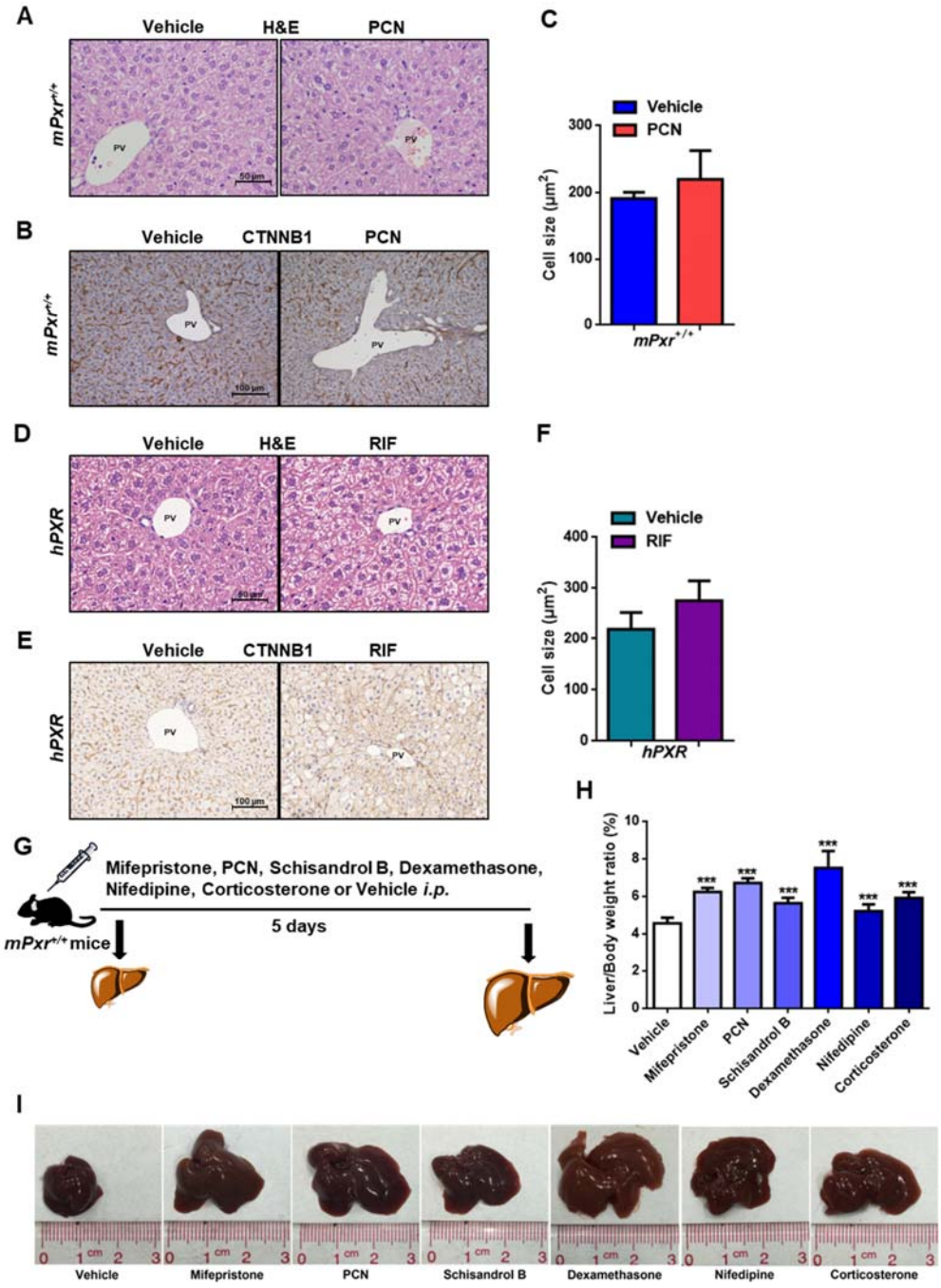

Figure S2. Effects of PXR activation on liver enlargement and liver cell size. (A-C) H&E and CTNNB1 staining of portal vein areas in PCN-treated WT mice (Membrane CTNNB1 staining was performed to describe the cell size) (n = 3). (D-F) H&E and CTNNB1 staining of portal vein areas in RIF-treated *hPXR* mice (n = 3). (G) Mice were treated with some PXR activators such as mifepristone (100 mg/kg/d), PCN (100 mg/kg/d), schisandrol B (100 mg/kg/d), dexamethasone (50 mg/kg/d), nifedipine (50 mg/kg/d), corticosterone (50 mg/kg/d) for 5 days. (H) Liver-to-body-weight ratios were shown. Data were expressed as means ± SD (n = 6). $^{***}P$<0.001 compared to vehicle

group. (I) Representative gross pictures of mouse livers after a 5-day treatment of the above PXR activators.

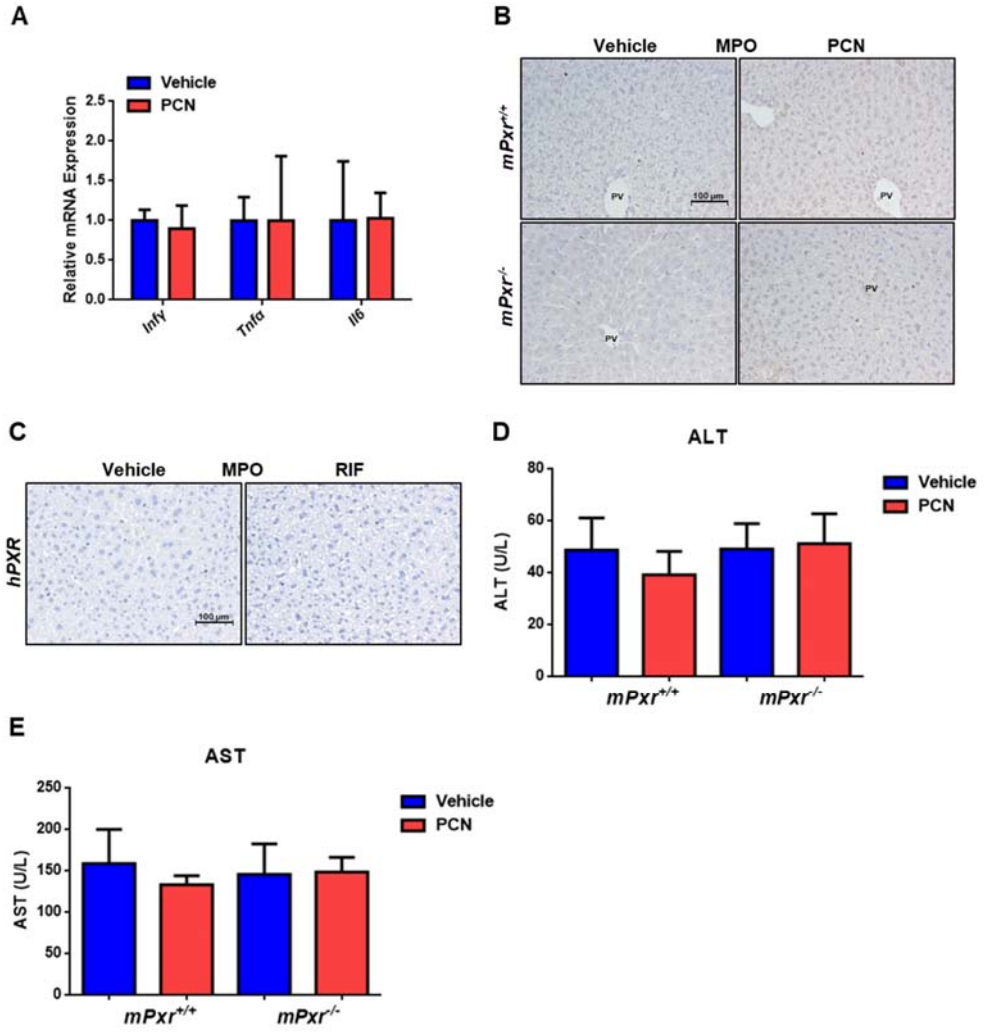

Figure S3. Biochemical and inflammation parameters. (A) qRT-PCR analysis of *Infγ*, *Tnfα* and *Il6* mRNA levels in livers after a 5-day treatment of PCN in WT mice. (B) IHC showing MPO staining in WT and *Pxr*-null mice. (C) IHC staining of MPO in *PXR*-humanized (*hPXR*) mice. (D-E) Serum ALT and AST levels after PCN treatment in WT and *Pxr*-null mice. Data were expressed as means ± SD (n = 6).

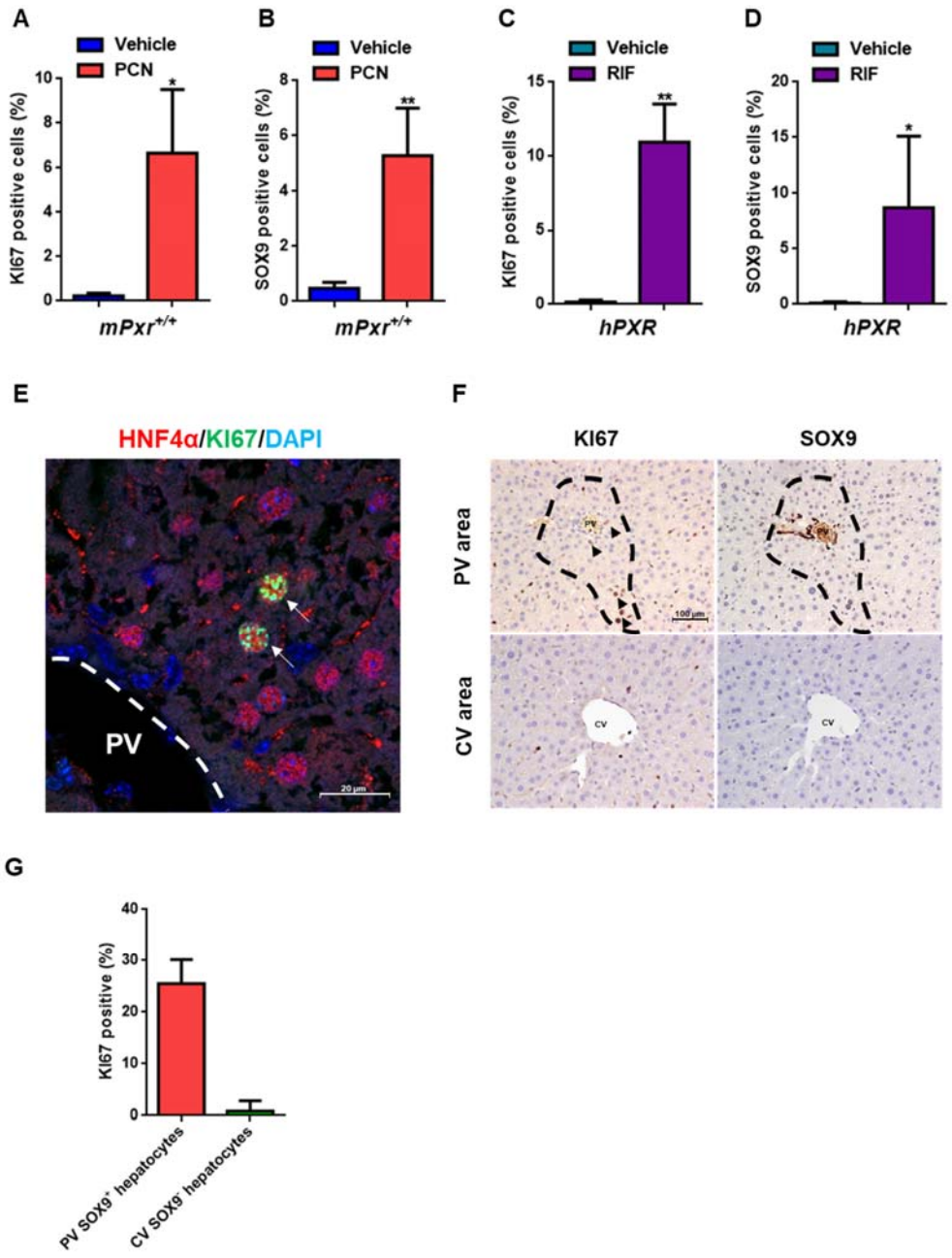

Figure S4. PXR activation induced hepatocytes proliferation and hybrid periportal hepatocytes. (A-D) Quantification of SOX9 and KI67 positive cells in WT and *hPXR* mice (n = 3). (E) HNF4α and KI67 double staining in PCN-treated mice. (F) Series section of KI67 and SOX9 IHC staining of portal and central vein areas in PCN-treated mice. (G) Quantification of KI67 positive cells in PV $SOX9^{+}$ and CV $SOX9^{-}$ cells. The data are expressed as the means ± SD. $^{*}P < 0.05$ and $^{**}P<0.01$ compared with the vehicle group.

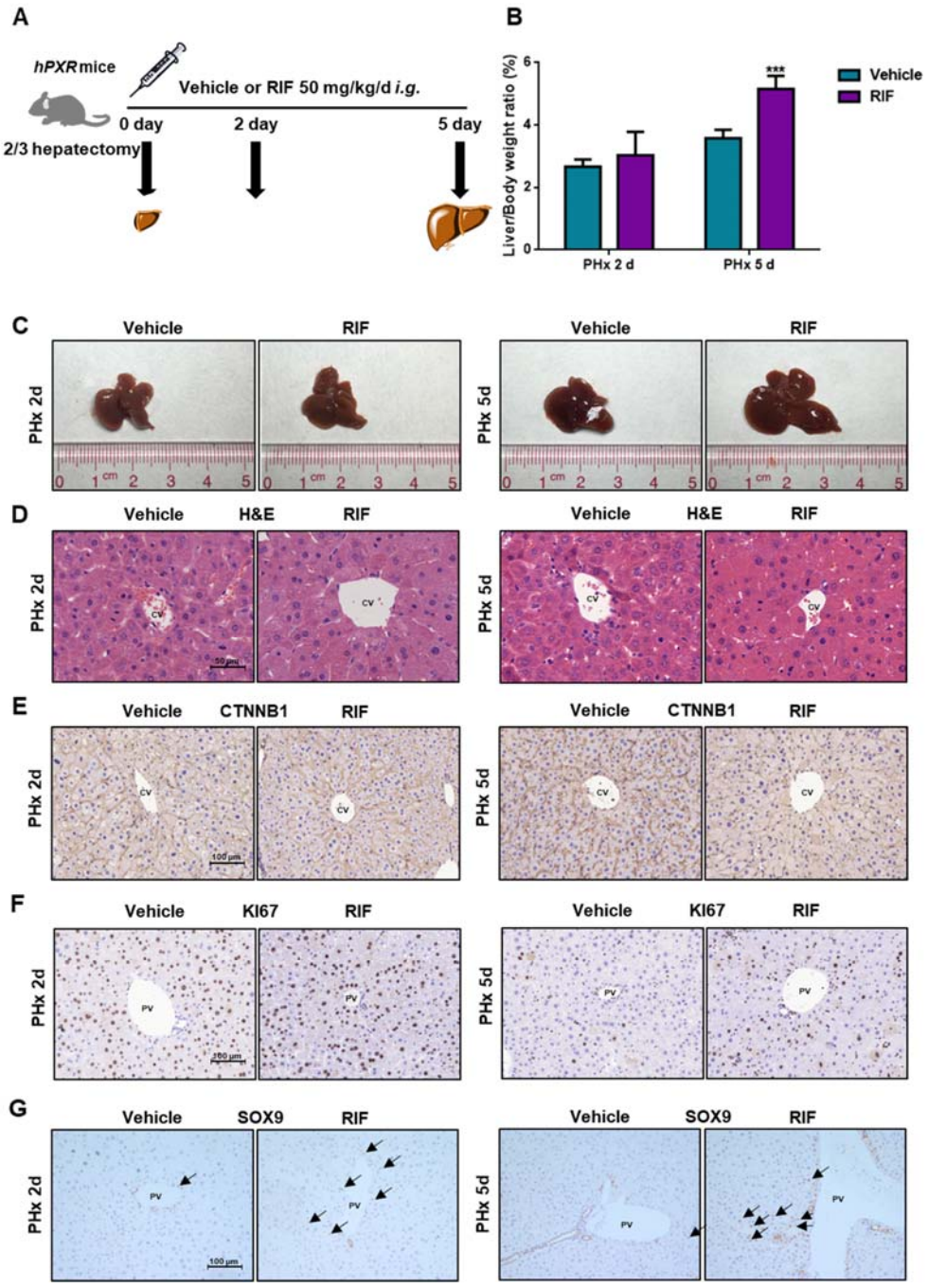

Figure S5. Effects of PXR activation on liver regeneration after PHx in *hPXR* mice. (A) *hPXR* mice were treated with RIF or vehicle following surgery and sacrificed at day 2 and day 5. (B) Liver-to-body-weight ratios. The data are expressed as the means ± SD (n = 4). $^{***}P<0.001$ compared with the vehicle group at the same time point. (C) Representative gross pictures of mouse livers after RIF administration for 2 days and 5 days. (D-G) Histopathological and IHC staining of representative mouse liver samples following H&E (D), CTNNB1 (E), KI67 (F), and SOX9 (G) staining.

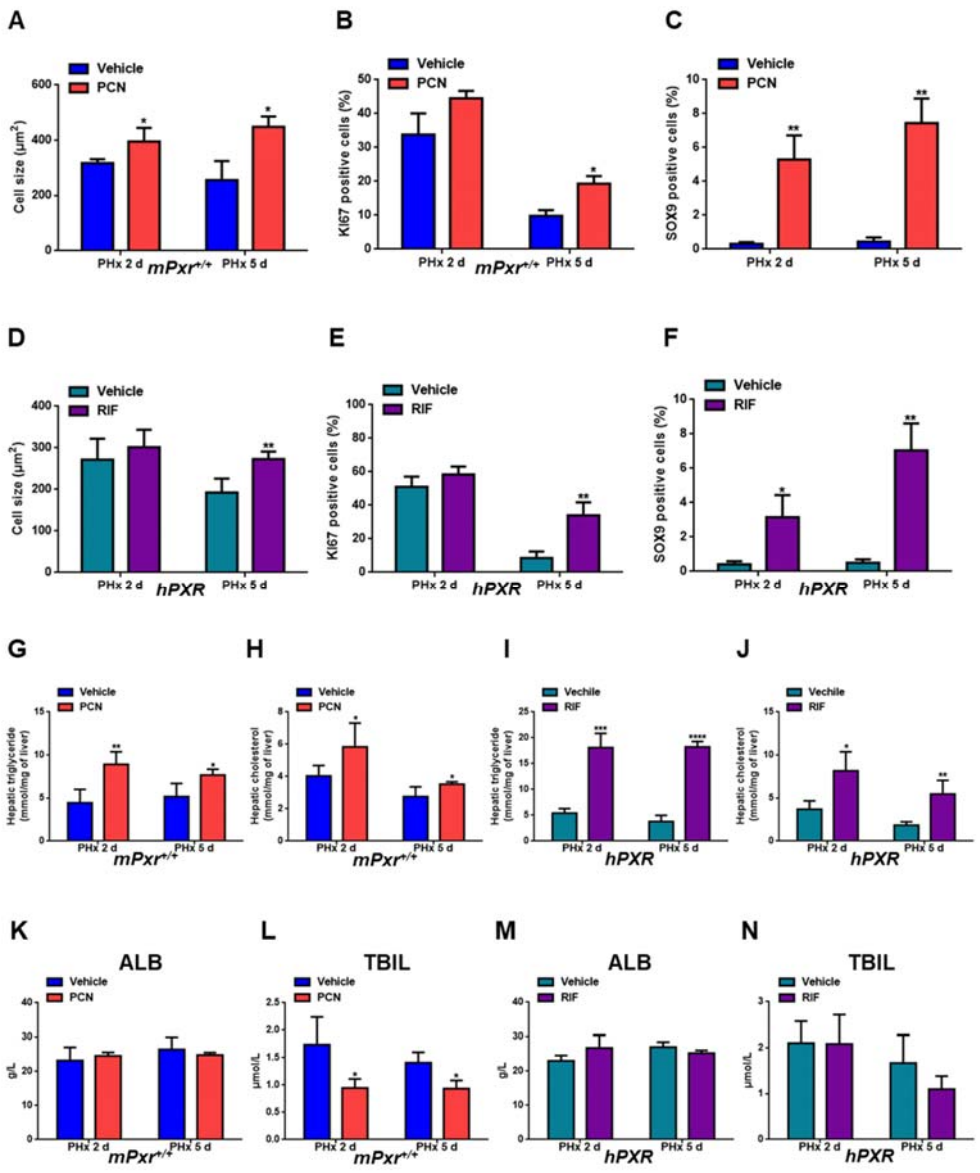

Figure S6. Effect of PXR activation on liver regeneration after PHx. (A-C) Quantification of cell size (A) , KI67$^+$ (B) and SOX9$^+$ (C) cells in WT mice at day 2 and day 5 PHx. (D-F) Quantification of cell size (D) , KI67$^+$ (E) and SOX9$^+$ (F) cells in *hPXR* mice at day 2 and day 5 PHx. (G-H) Hepatic triglyceride (G) and cholesterol (H) levels in WT mice at day 2 and day 5 PHx. (I-J) Hepatic triglyceride (I) and cholesterol (J) levels in *hPXR* mice at day 2 and day 5 PHx. (K-N) Serum ALB (K) and TBIL (L) levels in WT mice at day 2 and day 5 PHx. (M-N) Serum ALB (M) and TBIL (N) levels in *hPXR* mice at day 2 and day 5 PHx. The data are expressed as the means ± SD. $^*P < 0.05$, $^{**}P < 0.01$, $^{***}P < 0.001$ and $^{****}P<0.0001$ compared with the vehicle group.

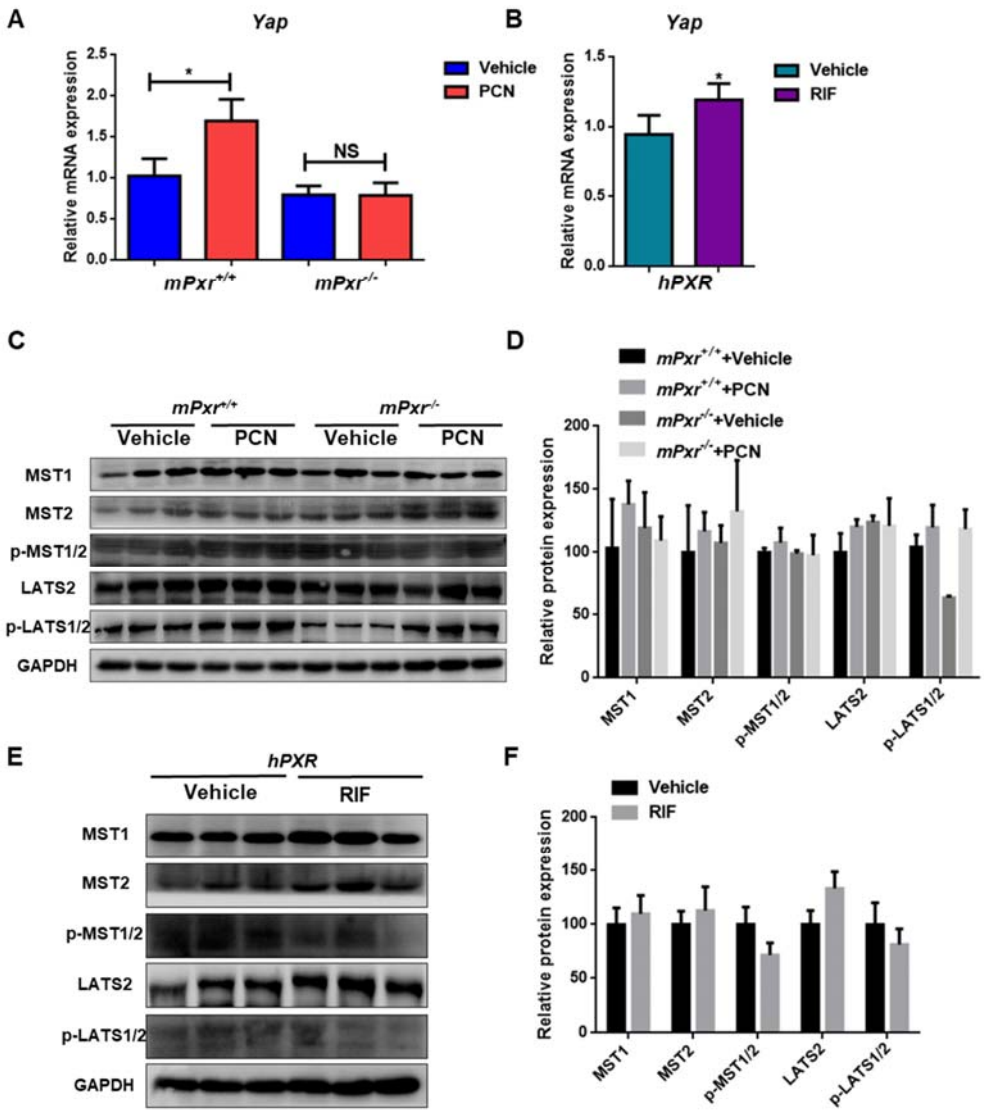

Figure S7. Effects of PXR activation on YAP pathways. (A) The expression of *Yap* in WT and *Pxr*-null mice (n = 6). (B) The expression of *Yap* in *hPXR* mice (n = 4). The data are expressed as the means ± SD. $^{*}P < 0.05$ compared with the vehicle group. (C-D) Western blot analysis of YAP upstream protein in WT and *Pxr*-null mice. (E-F) Western blot analysis of YAP upstream protein in *hPXR* mice.

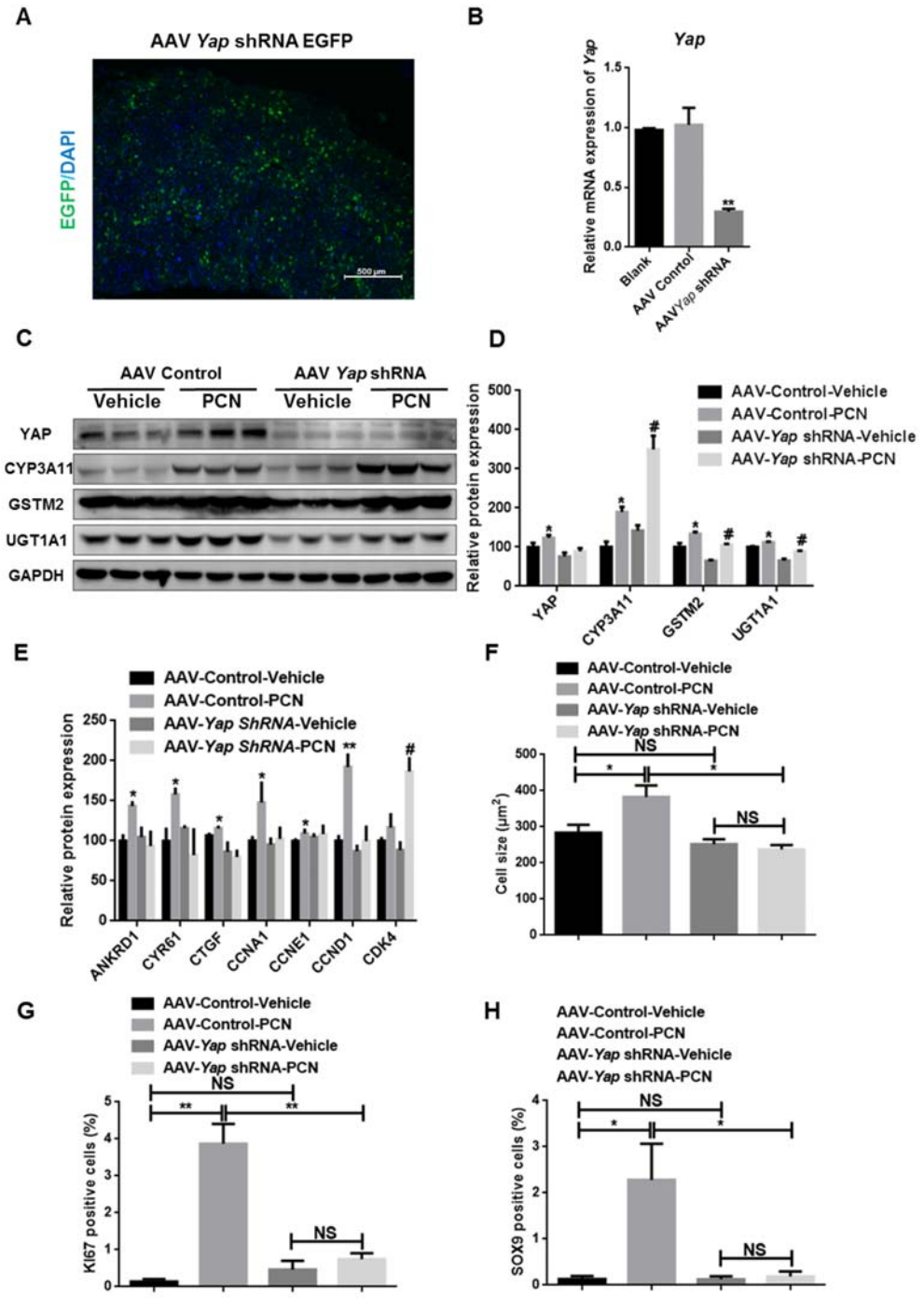

Figure S8. Effects of PXR activation with *Yap* interference. (A) EGFP stain of representative slides from AAV *Yap* shRNA EGFP mice. (B) qRT-PCR analysis was performed to measure gene expression of *Yap* after AAV *Yap* shRNA administration in AML12 (n=3). (C-E) Western blot was used to measure PXR and YAP downstream protein expression in AAV-Control and AAV *Yap* shRNA mice (n = 5). (F-H)

Quantification of cell size (F), KI67^{+} (G), and SOX9^{+} cells (H) in AAV-Control and AAV *Yap* shRNA mice. Data were expressed as means ± SD (n = 3). $^{*}P<0.05$ and $^{**}P<0.01$ compared to the control group.

Table S1. Sequences of primers and probes for quantitative real-time PCR

Genes	Primers (5'-3') Forward	Primers (5'-3') Reverse
Infγ	ATGAACGCTACACACTGCATC	CCATCCTTTTGCCAGTTCCTC
Tnfα	CCCTCACACTCAGATCATCTTCT	GCTACGACGTGGGCTACAG
Il6	TAGTCCTTCCTACCCCAATTTCC	TTGGTCCTTAGCCACTCCTTC
Yap	ACCCTCGTTTTGCCATGAAC	TGTGCTGGGATTGATATTCCGTA
Gapdh	AGGTCGGTGTGAACGGATTTG	GGGGTCGTTGATGGCAACA

References

1. Pascussi JM, Robert A, Nguyen M, Walrant-Debray O, Garabedian M, Martin P, Pineau T, et al. Possible involvement of pregnane X receptor-enhanced CYP24 expression in drug-induced osteomalacia. J Clin Invest 2005;115:177-186.
2. **Hu J, Srivastava K**, Wieland M, Runge A, Mogler C, Besemfelder E, Terhardt D, et al. Endothelial cell-derived angiopoietin-2 controls liver regeneration as a spatiotemporal rheostat. Science 2014;343:416-419.
3. Furuyama K, Kawaguchi Y, Akiyama H, Horiguchi M, Kodama S, Kuhara T, Hosokawa S, et al. Continuous cell supply from a Sox9-expressing progenitor zone in adult liver, exocrine pancreas and intestine. Nat Genet 2011;43:34-41.
4. **Zeng H, Jiang Y**, Chen P, Fan X, Li D, Liu A, Ma X, et al. Schisandrol B protects against cholestatic liver injury through pregnane X receptors. Br J Pharmacol 2017;174:672-688.
5. **Jiang Y, Fan X**, Wang Y, Chen P, Zeng H, Tan H, Gonzalez FJ, et al. Schisandrol B protects against acetaminophen-induced hepatotoxicity by inhibition of CYP-mediated bioactivation and regulation of liver regeneration. Toxicol Sci 2015;143:107-115.
6. Klaunig JE, Goldblatt PJ, Hinton DE, Lipsky MM, Chacko J, Trump BF. Mouse liver cell culture. I. Hepatocyte isolation. In Vitro 1981;17:913-925.